BIOCHEMISTRY
including biophysical chemistry & molecular biology
Article

*Biochemistry* **2009,** *48,* 6633–6643 6633
DOI: 10.1021/bi900564k

# Human Replication Protein A−Rad52−Single-Stranded DNA Complex: Stoichiometry and Evidence for Strand Transfer Regulation by Phosphorylation†

Xiaoyi Deng,[‡,§,⊥] Aishwarya Prakash,[‡,⊥] Kajari Dhar,[‡] Gilson S. Baia,[‡] Carol Kolar,[‡] Greg G. Oakley,[∥] and Gloria E. O. Borgstahl*[,‡]

[‡]*The Eppley Institute for Research in Cancer and Allied Diseases and* [§]*Department of Biochemistry and Molecular Biology, University of Nebraska Medical Center, 987696 Nebraska Medical Center, Omaha, Nebraska 68198-7696, and* [∥]*College of Dentistry, University of Nebraska Medical Center, 40th and Holdrege, Lincoln, Nebraska 68583-0740*
[⊥]*These authors contributed equally to this work*

*Received April 2, 2009; Revised Manuscript Received May 19, 2009*

ABSTRACT: The eukaryotic single-stranded DNA-binding protein, replication protein A (RPA), is essential in DNA metabolism and is phosphorylated in response to DNA-damaging agents. Rad52 and RPA participate in the repair of double-stranded DNA breaks (DSBs). It is known that human RPA and Rad52 form a complex, but the molecular mass, stoichiometry, and exact role of this complex in DSB repair are unclear. In this study, absolute molecular masses of individual proteins and complexes were measured in solution using analytical size-exclusion chromatography coupled with multiangle light scattering, the protein species present in each purified fraction were verified via sodium dodecyl sulfate−polyacrylamide gel electrophoresis (SDS−PAGE)/Western analyses, and the presence of biotinylated ssDNA in the complexes was verified by chemiluminescence detection. Then, employing UV cross-linking, the protein partner holding the ssDNA was identified. These data show that phosphorylated RPA promoted formation of a complex with monomeric Rad52 and caused the transfer of ssDNA from RPA to Rad52. This suggests that RPA phosphorylation may regulate the first steps of DSB repair and is necessary for the mediator function of Rad52.

Double-strand breaks (DSBs)[1] in chromosomal DNA are efficiently repaired by homologous recombination (HR) (*1*). The RAD52 epistasis group of proteins, including Rad51, Rad52, and replication protein A (RPA), performs the repair of DSBs by HR (*2*, *3*). Studies with *Saccharomyces cerevisiae* proteins (*4*−*6*) and with human proteins (*7*−*10*) demonstrated the importance of specific protein−protein contacts in controlling the functional interactions among Rad51, Rad52, and RPA. Rad52 acts as a mediator between RPA-coated ssDNA and Rad51 (*11*−*13*), and a similar function is also proposed for human BRCA2 protein (*14*). However, the molecular mechanisms for the delivery of Rad51 by mediators to RPA-coated ssDNA are not known in detail.

RPA is the ubiquitous eukaryotic single-stranded DNA (ssDNA) binding protein that is composed of three subunits that have been named for their molecular masses in kilodaltons as RPA70, RPA32, and RPA14 (*15*, *16*). The heterotrimer is the main biological form of RPA (*17*, *18*) and is very stable when purified (*19*). RPA binds ssDNA more tightly than RNA or double-stranded DNA (dsDNA), prefers purines over pyrimidines (*16*), and has a 25−30-nucleotide footprint (*20*). RPA is composed of six oligonucleotide/oligosaccharide binding (OB) domains that bind ssDNA and/or participate in specific protein−protein interactions (*21*). RPA is also known to undergo a significant conformational change upon binding DNA (*22*, *23*) that appears to alter RPA's structure in a way that facilitates interactions with other proteins and ssDNA.

The exact signal(s) for the presence of single- or double-stranded DNA breaks in a cell is still poorly understood, but the ssDNA−RPA complex appears to be an important component (*24*). Once DSBs are sensed, several downstream HR repair effector proteins are phosphorylated (*25*). RPA is phosphorylated (and dephosphorylated) during the cell cycle, in response to DNA damage and during apoptosis (*26*−*33*). Most studies have focused on the phosphorylation of the N-terminus of RPA32, and up to nine Ser/Thr sites have been identified in the first 33 amino acids. Chromatin-associated fractions of RPA contain the phosphorylated forms of RPA32, and phosphorylation can cause

†This work was supported by the U.S. Army Medical Research and Materiel Command under Contract DAMD17-98-1-8251 (G.E.O.B.), American Cancer Society Grant RSG-02-162-01-GMC (G.E.O.B.), and National Cancer Institute Eppley Cancer Center Support Grant P30CA036727.

*To whom correspondence should be addressed. Telephone: (402) 559-8578. Fax: (402) 559-3739. E-mail: gborgstahl@unmc.edu.

[1]Abbreviations: RPA, replication protein A; pRPA, phosphorylated RPA; RPA70, 70 kDa subunit of RPA; RPA32, 32 kDa subunit of RPA; RPA14, 14 kDa subunit of RPA; ssDNA, single-stranded DNA; dsDNA, double-stranded DNA; DSBs, double-stranded DNA breaks; HR, homologous recombination; UV, ultraviolet; LS, light scattering; IR, interferometric refractometer; ELISA, enzyme-linked immunosorbent assay; SEC−MALS, size-exclusion chromatography with multiangle light scattering.


Published on Web 06/16/2009

the RPA heterotrimer to dissociate (*34*). RPA is known to be phosphorylated upon exposure of cultured human cells to UV or ionizing radiation (*30*, *33*). This DNA damage-induced phosphorylation is coincident with cell cycle arrest and loss of the ability of cell extracts to support DNA replication (*33*). It is known that ATM kinase, DNA-dependent protein kinase, and cyclin-Cdk phosphorylate RPA32 N-terminal residues (*26*, *35*, *36*). Recent studies have revealed new phosphorylation sites on RPA32 and RPA70 and that phosphorylation modulates the affinity of RPA for ssDNA (*37*−*39*). The localization of phosphorylated RPA (pRPA) to other DSB repair proteins, including Rad52, has been reported (*24*), and pRPA facilitates chromosomal DNA repair in cells (*36*). An improved interaction between RPA and Rad52 was observed by immunoprecipitation following hydroxyurea treatment (known to produce pRPA), and cell cycle regulators (like Chk1) are thought to lead to replacement of RPA with Rad51 and Rad52 during HR (*40*). These observations suggest that phosphorylation serves as an essential mechanism for modulating RPA's activity, its quaternary structure, and its interactions with other proteins. Although the effects of pRPA on DNA replication and various DNA repair pathways have been studied (*28*), limited information about the regulation of the protein−protein and protein−DNA complexes involved in DSB repair by pRPA is available.

Rad52 protein has three known activities in DSB repair (*13*, *41*). The first activity is early in the mechanism and involves the recruitment of Rad51 onto ssDNA that is coated with RPA at the break site. This is a well-characterized and essential function of Rad52 for the in vivo function of Rad51 in yeast (*11*) and appears to be a function that may overlap with BRCA2 protein in humans (*42*). The second activity is to anneal complementary ssDNA molecules that have RPA bound in the single-strand annealing pathway for DSB repair in regions of repetitive DNA sequences (*43*). This mutagenic pathway is stimulated when BRCA2 is deficient (*44*, *45*) and promotes genomic instability. The third activity is downstream of Rad51-mediated DNA strand exchange where Rad52 promotes the annealing of the displaced ssDNA strand to a second ssDNA strand (*13*, *41*). Rad52 has greater binding affinity for ssDNA than dsDNA (*46*, *47*) and appears to have two separate binding sites for each in the N-terminus of Rad52 (*48*). Studies have shown that Rad52 has a binding preference for 5′ or 3′ ssDNA ends, and ssDNA hypersensitivity to hydroxyl radical patterns suggests that four nucleotides are protected by Rad52 binding (*49*, *50*). Rad52 is capable of capping DNA termini, can protect DSBs from nuclease attack (*46*, *49*) after the ends are processed into ssDNA tails (*51*), and can promote ligation (*49*, *52*). Electron microscopy (EM) studies of *S. cerevisiae* and hRad52 have revealed formation of ring-shaped structures (9−13 nm in diameter), as well as higher-order aggregates (*49*, *53*−*55*). Structural and solution studies have demonstrated that the self-association domain in the N-terminal half of Rad52 is responsible for ring formation and that elements in the C-terminal half of the molecule participate in the formation of higher-order complexes of rings (*56*, *57*). Human Rad52 rings in EM analysis have been interpreted to be composed of seven subunits (*56*, *57*), whereas crystal structures of the N-terminal half of human Rad52 revealed an undecameric ring (*58*, *59*). The function of Rad52 multimers remains unclear, although multimerization appears to be important for nuclear localization (*60*). Singleton and co-workers speculated that ssDNA binds in a positively charged groove and wraps around the ring (*59*). The stoichiometry of RPA and Rad52 complexes and the effects of protein−protein interactions on DNA specificity and affinity are not well understood and are the topic of this study.

Human RPA and Rad52 have specific interactions with each other (*61*−*66*). The interaction of Rad52 with RPA was shown to significantly increase the affinity of RPA for homopurine ssDNA in vitro (*62*) which is counterintuitive for Rad52's mediator function. However, the effect of pRPA on Rad52 intermolecular interactions has not been explored. In this study, we explored the effects of pRPA on Rad52 protein−protein and DNA−protein complexes. We conducted a series of stoichiometry experiments with purified components in solution by measuring absolute molecular masses of individual proteins as well as DNA−protein complexes with analytical size-exclusion chromatography coupled with multiangle light scattering (SEC−MALS) (see refs *67* and *68* for reviews of the SEC−MALS methodology). Our results indicate that pRPA interacts differently with ssDNA and Rad52. It also reveals that the affinity of Rad52 for ssDNA increases when pRPA is part of the complex and indicates transfer of ssDNA from pRPA to Rad52. On the basis of these data, we propose a model for the initial steps in HR-based DSB repair. In these studies, we have also tested the relevance of the Rad52 ring model in DSB repair. The data reported indicate the importance of both pRPA and monomeric Rad52 in DSB repair in humans.

## EXPERIMENTAL PROCEDURES

*Protein Purification, Phosphorylation, and ssDNA*. Rad52 proteins (*57*, *62*) and RPA proteins (*69*) were purified as described previously with the following modification. Bacterial cultures expressing recombinant RPA were supplemented with 100 $\mu$M $ZnCl_2$. The protein concentrations were calculated using a Bradford assay (Bio-Rad) with bovine serum albumin as a standard. pRPA was prepared in vitro and purified as previously described and characterized (*37*, *39*). Briefly, RPA was purified as above and for phosphorylation, the RPA was dialyzed and mixed with HeLa extracts. The mixture was supplemented with an ATP regenerating system, ssDNA, and phosphatase inhibitors to inhibit phosphatase activity within the cell extracts. This reaction allows for endogenous kinases within the HeLa extract to phosphorylate RPA. Following incubation for 3 h at 30 °C, the hyperphosphorylated RPA was purified in a manner identical to that of recombinant RPA, mentioned above. The ionic strength of buffer solutions was optimized and kept as low as possible to support protein complex formation as well as protein solubility (see Figure 7 of ref *62*). Thus, RPA was dialyzed against buffer A [50 mM Tris (pH 7.8), 0.5% inositol, 2 mM EDTA, 2 mM 2-mercaptoethanol, and 150 mM KCl; note that the KCl concentration varied as specified], and Rad52 was dialyzed against buffer A with 200 mM KCl. The 3′-biotinylated synthetic 25mer oligonucleotide was designed based on a natural DNA gene sequence, using DNASTAR to minimize secondary structure and dimers, and was composed of the sequence GCTAGCTCAATTCATCGACAAACCT ($M_W$ = 7815 Da). Biotinylated oligonucleotide was dissolved in water, and the concentration was measured at $OD_{260}$ using an extinction coefficient of 4.21 $nM^{-1}$ $cm^{-1}$.

*In Vitro Complex Formation*. We formed the ssDNA−RPA complex by mixing RPA and ssDNA at a 1:2 molar ratio in buffer A and incubating the mixture for 1 h on ice. We formed the

ssDNA−Rad52 complex by mixing ssDNA and Rad52 in a 2:1 ratio in buffer A with 200 mM KCl and incubating the mixture for 1 h on ice. We formed the RPA−Rad52 complex by mixing RPA and Rad52 in a 1:2 ratio in buffer A with 175 mM KCl. For the ssDNA−RPA−Rad52 complex, the ssDNA−RPA complex was mixed first and incubated for 1 h on ice and then Rad52 was added at a 2:1 ratio (Rad52:RPA) in buffer A. The ssDNA−pRPA−Rad52 complex was formed following the same protocol. All protein−protein complexes were incubated on ice overnight before being analyzed.

*Size-Exclusion Chromatography with Multiangle Light Scattering (SEC−MALS)*. SEC−MALS experiments were performed at room temperature by loading 100−240 μg of protein sample on a Superose 6 10/300 GL column (Amersham Biosciences) with a bed volume of approximately 24 mL, an exclusion limit of $4 \times 10^4$ kDa, and an optimal separation range from 5 to $5 \times 10^3$ kDa. A flow rate of 0.3 mL/min was used, unless otherwise indicated, using an Agilent HPLC instrument. The column was eluted with buffer A. Downstream from the column, a UV detector (Agilent), a miniDAWN triple-angle light scattering detector (Wyatt Technology), and an Optilab DSP interferometric refractometer (IR, Wyatt Technology) were connected in series. The refractometer provided a continuous index of protein concentration. A d*n*/d*c* (refractive index increment) value of 0.185 mL/mg was used. Bovine serum albumin was used as an isotropic scatterer for detector normalization. The light scattered by a protein is directly proportional to its weight-average molecular mass and concentration. Therefore, molecular masses ($M_W$) were calculated from the light scattering and IR concentration data using Astra. Error in SEC−MALS measurements can be caused by a relatively low concentration of some species, interdetector band broadening, or poor $M_W$ separation that results in polydispersity of the sample as it flows through the downstream detectors. A low concentration gives a lower light scattering signal and causes a spread in the derived $M_W$ data. The chromatograms from the LS and IR detectors do not overlay when there is polydispersity in the samples. Polydispersity is also indicated by the breadth and shape of the peaks in the chromatogram. The derived $M_W$ data will have a sloped appearance for polydisperse samples and can appear to grin or frown due to interdetector band broadening. Fractions (0.1 mL) collected were analyzed by sodium dodecyl sulfate−polyacrylamide gel electrophoresis (SDS−PAGE), chemiluminescent ssDNA detection, antiRad52 Western blotting, and/or electron microscopy. The relative areas of IR peaks were manually calculated.

*Chemiluminescence ssDNA Detection and UV Cross-Linking*. For each SEC−MALS peak, 1 μL of every fraction was dotted on a nylon membrane (0.45 μm, Invitrogen) and biotinylated ssDNA was detected by chemiluminescence (Chemiluminescent Nucleic Acid Detection Module, Pierce), according to the manufacturer's protocol. In some experiments, ssDNA was cross-linked to protein via a 2 min exposure in a UV Stratalinker 1800, before SDS−PAGE separation and detection by chemiluminescence.

*Gel Mobility Shift Assays*. Individual DNA binding reaction mixtures (10 μL) containing 10 mM Tris (pH 7.5), 150 mM KCl, 1 mM DTT, 5% (v/v) glycerol, 100 fmol of ssDNA, and a varying amount of RPA (0−300 fmol) were incubated at room temperature for 20 min. Then 3 μL of DNA loading buffer [150 mM Tris (pH 6.8), 300 mM DTT, 0.1% bromophenyl blue, and 30% glycerol] was added to each reaction mixture, and the entire mixture was separated by electrophoresis at 70 V for ~45 min at 4 °C on native 4% agarose gels in 1× TAE buffer. The gels were transferred onto a positively charged nylon membrane and UV cross-linked for 1 min, and ssDNA was detected by chemiluminescence (using the Chemiluminescence EMSA kit from Pierce).

*SDS−PAGE Analysis and Rad52 Western Blots*. For each SEC−MALS peak, 10 μL of each fraction was mixed with 5 μL of SDS loading buffer [150 mM Tris-HCl (pH 6.8), 300 mM DTT, 6% SDS, 0.3% bromophenol blue, and 30% glycerol], boiled in a water bath for 3 min, briefly centrifuged, loaded on a NuPAGE 10% Bis-Tris gel (Invitrogen), and separated by SDS−PAGE. Duplicate gels were run. One was silver stained, and the other was analyzed by Western blotting. Proteins were transferred to a nitrocellulose membrane (Invitrogen) and probed with mouse anti-Rad52 antibody specific for human Rad52 residues 303−340 (antibody #207 as described in ref *62*).

*Electron Microscopy (EM)*. All protein peaks from SEC−MALS fractions that could possibly contain Rad52 were examined by EM. Only those samples that indicated clearly defined structures are discussed in the text and summarized in Table 1. Samples for EM were prepared by dilution to 2.0 μM in buffer A with 200 mM KCl. Samples were spread onto thin carbon films on 400 mesh carbon grids, stained with 1% uranyl acetate, and visualized by transmission electron microscopy using a Philips 410LS transmission electron microscope.

## RESULTS

*ssDNA−RPA−Rad52 Complex*. The molecular masses of purified RPA and Rad52 protein samples and their ssDNA complexes were measured by SEC−MALS analysis for direct molecular mass determination. With SEC−MALS, the intensity of light scattered is directly proportional to molecular mass, and when these are combined with protein concentration data provided by the interferometric refractometer, the absolute molecular mass can be determined for homogeneously separated species.

The form of RPA relevant to DNA repair has ssDNA bound, so the effect of prebinding RPA with a short piece of ssDNA on the stoichiometry of a RPA−Rad52 complex was analyzed by SEC−MALS (Figure 1). Four species were defined for the ssDNA−RPA−Rad52 mixture (Table 1, sample 1): (1) minor amounts of a 1034 kDa structure composed of Rad52 (in excess), ssDNA, and RPA (Figure 1B, lanes 3−9), (2) minor amounts of a 356.9 kDa complex composed of equal amounts of Rad52, ssDNA, and RPA (Figure 1B, lanes 11−13), (3) major amounts of a 142.1 kDa mixture of excess RPA, ssDNA, and Rad52 monomer (Figure 1B, lanes 14−16), and (4) minor amounts of a lower-molecular mass species containing RPA, excess ssDNA, and Rad52 (Figure 1B, lanes 17−21). Peaks 1 and 2 were examined by EM, but ring-shaped aggregates were not observed. Western analysis indicates that Rad52 is present in all fractions at all molecular masses. When RPA was pretreated with $dT_{25}$ in similar experiments, the RPA-Rad52 complex was barely detectable (data not shown), indicating that the sequence of the oligonucleotide may have an effect on the formation of a protein−protein complex. Thus, the Rad52 ring structure may be disrupted in the ssDNA−RPA−Rad52 complex.

Our previous studies indicated that the RPA−Rad52 complex increased the affinity of RPA for ssDNA (*62*). Thus, to determine which protein partner is bound to the ssDNA in the complexes,

Table 1: Summary of SEC−MALS, SDS−PAGE, Western Blot, and EM Results

| sample[a] | measured molecular[b] mass ($M_W$) (kDa) for each peak on the chromatogram | ssDNA detected | Rad52 detected by Western blot | rings visible by EM | ssDNA cross-linked | interpretation from combined data, including SDS−PAGE analysis[f] |
|---|---|---|---|---|---|---|
| (1) ssDNA−RPA + Rad52 | peak 1, 1034 (2.5, 1.015) | + | + | − | − | ~3 RPA + excess Rad52 + ssDNA (Rad52 in excess on gel) |
| | peak 2, 356.9 (3.0, 1.005) | + | + | − | ± | 2RPA + 2Rad52 monomers + ssDNA (1:1 RPA:Rad52 on gel) |
| | peak 3, 142.1 (0.8, 1.002) | + | + | − | + | RPA + Rad52 monomer + ssDNA (RPA in excess on gel) |
| | peak 4, nd[c,d] | + | + | − | + | RPA + Rad52 monomer + ssDNA in excess (1:1 RPA:Rad52 on gel) |
| (2) ssDNA−pRPA + Rad52 | peak 1, 966.4 (2.1, 1.005) | + | | | − | RPA + Rad52 + ssDNA (Rad52 in excess on gel) |
| | peak 2, 136 (1.6, 1.001) | + | | | + | RPA + Rad52 monomer + ssDNA (1:1 RPA:Rad52 on gel) |
| | peak 3, nd[c,d] | + | | | − | RPA + Rad52 monomer + ssDNA in excess |
| (3) RPA + Rad52 | peak 1, 706.9 (0.8, 1.012) | | + | +[e] | | 1 RPA + excess Rad52 (RPA weak on gel) |
| | peak 2, 154.4 (1.5, 1.005) | | + | − | | RPA + Rad52 monomer (RPA in excess on gel) |
| | peak 3, nd[c,d] | | + | − | | RPA + Rad52 monomer (1:1 RPA:Rad52 on gel) |
| (4) RPA | peak 1, 111.0 (0.4, 1.000) | | | | | 110.8 kDa RPA |
| (5) ssDNA−RPA | peak 1, 380.3 (23, 1.022)[d] | + | | | | aggregates of RPA and ssDNA |
| | peak 2, 125.1 (3, 1.001) | + | | | | 110.8 kDa RPA + 2 × 7.8 ssDNA[g] |
| (6) Rad52 | peak 2, 538.9 (0.22, 1.002) | | | + | | 11 × 47.4 kDa Rad52 monomer |
| (7) ssDNA−Rad52 | peak 1, 634.9 (2.1, 1.003) | + | | +[e] | | 11 × 47.4 kDa Rad52 monomer + 12 × 7.8 kDa ssDNA |
| | peak 2, nd[c,d] | + | | − | | Rad52 monomer + ssDNA in excess |

[a] Corresponding chromatograms, detection of ssDNA, Rad52 Western, EM, and silver-stained SDS−PAGE analysis are given in Figures 1−5. [b] Weight-average molecular mass ($M_W$) data measured directly from light scattering using Astra version 4.90. Percent error and polydispersity are given in parentheses. The ratio $M_W/M_n$ gives a relative measure of polydispersity, where $M_n$ is the number-average molecular mass. The exclusion limit of the Superose 6 column is 40000 kDa, and the optimal separation range is 5−5000 kDa. [c] Not determined. [d] Large error due to poor light scattering; sparsely populated species and in particular smaller species have relatively poor light scattering. These sources of error limit the interpretation of high and low $M_W$ values. In these cases, the confirmation by SDS−PAGE and Western blots are particularly important. [e] Horseshoe structure determined by EM. [f] Interpretation is based on the $M_W$ predicted from the amino acid sequence using Edit Seq in the DNASTAR suite of software, silver-stained SDS−PAGE, Western blots of Rad52, and chemiluminescence analysis of biotin-labeled ssDNA. [g] The stoichiometry of RPA to oligo was further analyzed on a more appropriate SEC column (see the Supporting Information).

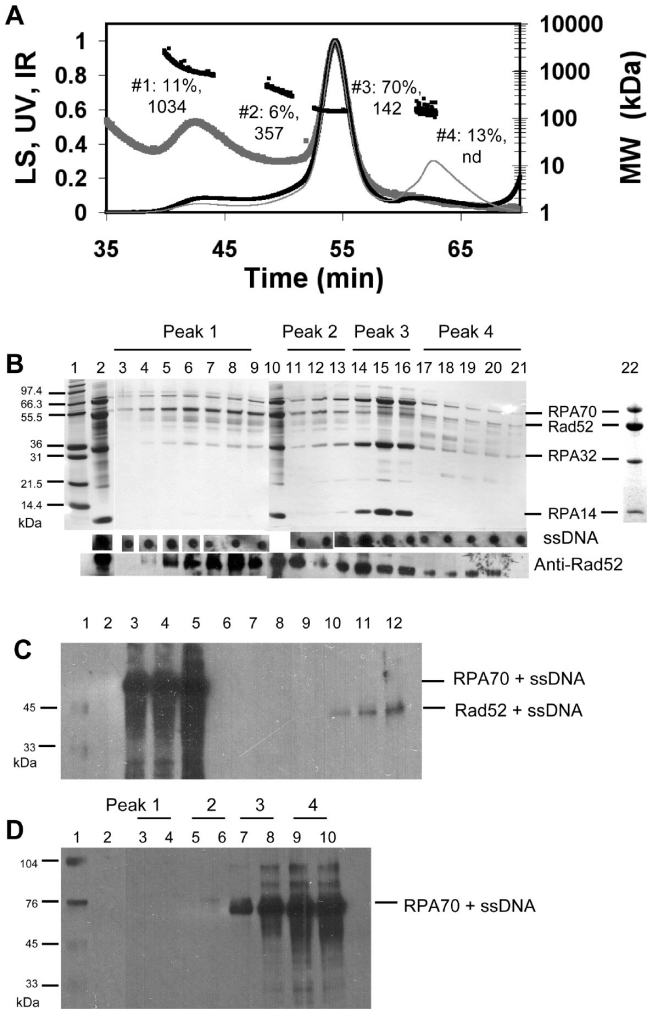


FIGURE 1: Analysis of the ssDNA−RPA−Rad52 complex. (A) SEC−MALS data of the ssDNA−RPA−Rad52 complex. (B) Silver-stained SDS−PAGE (top), ssDNA detection (middle), and Rad52 Western blots (bottom) of fractions from panel A: lane 1, Mark12 protein standard (Invitrogen) with the $M_W$ values in kilodaltons; lanes 2 and 10, input sample, 2.8 $\mu$g loaded; lanes 3−9, peak 1 fractions; lanes 11−13, peak 2 fractions; lanes 14−16, peak 3 fractions; lanes 17−21, peak 4 fractions; and lane 22, Coomassie stain of the input sample. (C) Controls. Detection of ssDNA cross-linked to individual proteins and separated by SDS−PAGE: lane 1, BlueRanger protein standard; lanes 2−5, ssDNA−RPA samples cross-linked for 0, 2, 5, and 20 min, respectively; lanes 6−8, ssDNA−BSA control samples cross-linked for 2, 5, and 20 min, respectively; and lanes 9−12, ssDNA−Rad52 samples cross-linked for 0, 2, 5, and 20 min, respectively. (D) Detection of ssDNA cross-linked (for 2 min) to protein and separated by SDS−PAGE of fractions from panel A: lane 1, BlueRanger; lane 2, input sample not cross-linked; lanes 3 and 4, peak 1 fractions; lanes 5 and 6, peak 2 fractions; lanes 7 and 8, peak 3 fractions; and lanes 9 and 10, peak 4 fractions. For the SEC−MALS data vs chromatographic elution time (in minutes) plots in all figures, the light scattering data are shown with a thick medium gray line, refractive index data are black, $A_{280}$ data are shows as a thin light gray line, and the derived absolute molecular masses ($M_W$) are represented by black squares above the peak regions. Please note that the relative population of species was calculated on the basis of peak areas of the refractive index data and are given next to the peak number. The $M_W$ in kilodaltons is also given for each peak. In this and other figures, all parts are from the same experiment.

the SEC fractions were treated with UV to cross-link protein to ssDNA and then separated by SDS−PAGE before the chemiluminescence detection of the biotin-labeled ssDNA. Control experiments show that both RPA70 and Rad52 can be cross-linked to ssDNA and are easily distinguishable in this assay (Figure 1C). Results were as follows. (1) For peak 1 (composed of mainly Rad52 multimers and ssDNA with low levels of RPA), no cross-linked ssDNA was detected (Figure 1D, lanes 3 and 4), although ssDNA was present in the fractions (Figure 1B, lanes 3−9). (2) For peak 2 (containing two RPA molecules, two Rad52 monomers, and ssDNA), cross-linking was weakly detected (Figure 1D, lanes 5 and 6). (3) For peak 3 (the major peak containing RPA, Rad52 monomer, and ssDNA) and peak 4 (possibly as individual subunits of RPA with ssDNA, Rad52 monomer with ssDNA, and excess ssDNA), ssDNA cross-linked to RPA70 (Figure 1D, lanes 7−10). These results indicate that in the lower-molecular mass complexes, mainly RPA70 has ssDNA bound. In the higher-molecular mass complexes, the ssDNA could not be cross-linked to any subunit of RPA or to Rad52. These results go along with our earlier observations that formation of the Rad52 complex increases the affinity of RPA for ssDNA (*62*).

*Effect of Phosphorylated RPA on the ssDNA−RPA−Rad52 Complexes*. Cellular RPA is phosphorylated in response to ionizing radiation, so a phosphorylated form of RPA is likely to be the active agent in HR-based DSB repair. Therefore, the effects of purified pRPA (Figure 2A) on the stoichiometry of the complexes were also analyzed by SEC−MALS (Figure 2B). Three species were defined for the ssDNA−pRPA−Rad52 mixture (Table 1, sample 2): (1) minor amounts of a 966.4 kDa structure composed of Rad52 (in excess), ssDNA, and pRPA (Figure 2C, lanes 3−8), (2) major amounts of a 136 kDa complex composed of monomeric Rad52, ssDNA, and pRPA (Figure 2C, lanes 10−17; note that pRPA is in excess but there is more monomeric Rad52 seen by silver-stained SDS−PAGE than when RPA is not phosphorylated in Figure 1B, lanes 14−16), and (3) lower-molecular mass species containing Rad52, ssDNA (in excess), and pRPA (Figure 2C, lanes 18−20). The Rad52 component of the ssDNA−pRPA−Rad52 complex in peak 2 was much easier to detect by SDS−PAGE (Figure 2C, lanes 14−17; note that Rad52 and RPA70 are nearly equally stained) than for the corresponding ssDNA−RPA−Rad52 peak 3 sample (Figure 1B, lanes 14−16). Thus, the ssDNA−pRPA−Rad52 complex is relatively more stable and is more homogeneously composed of one monomer of Rad52 and one pRPA heterotrimer.

Again, UV cross-linking was performed to determine which protein partner binds to the ssDNA in the complexes. Results were as follows. (1) For peak 1, no cross-linked ssDNA was detected (Figure 2D, lanes 3−5), although ssDNA was present in the fractions (Figure 2C, lanes 3−8). (2) In peaks 2 and 3, ssDNA cross-linked to both Rad52 and RPA70 (Figure 2D, lanes 6−9 and 10−12). This is similar to the ssDNA−RPA−Rad52 results (Figure 1), in that for the higher-molecular mass complexes the ssDNA could not be cross-linked to any subunit of RPA or Rad52. Interestingly, in the lower-molecular mass complexes, both RPA70 and Rad52 can be cross-linked with ssDNA (Figure 2D, lanes 6−9 and 10−12).

To help deconvolute the effects of phosphorylation and protein−protein interactions on ssDNA binding affinity, we measured the relative affinity of RPA and pRPA for oligonucleotides by a gel mobility shift assay. Previous studies had indicated that this purified form of pRPA had no difference in ssDNA binding to pyrimidine-rich sequences and decreased affinity for purine-rich ssDNA (*39*). Gel mobility shift assays with the mixed sequence 25mer oligomer used in these studies indicate that pRPA has a relative increase in ssDNA binding

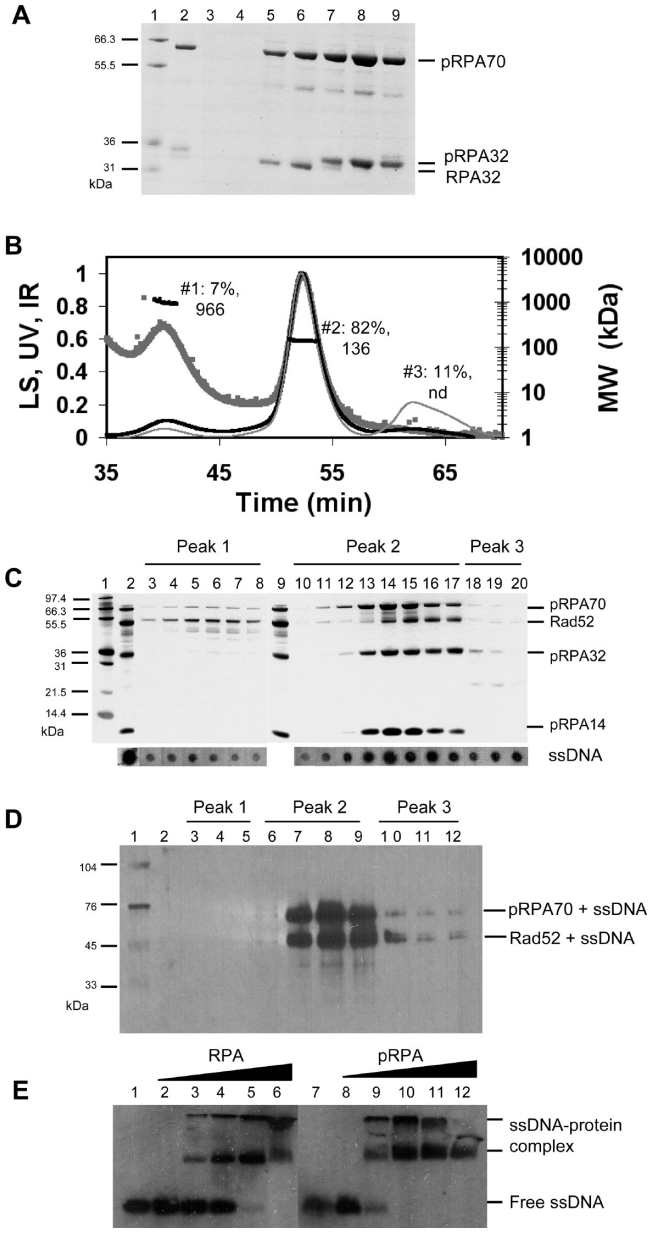


FIGURE 2: Analysis of the ssDNA−pRPA−Rad52 complex. (A) Purification of pRPA: lane 1, Mark12; lane 2, protein after hydroxyapatite; and lanes 3−9, fractions from the MonoQ column (fractions 8 and 9 were used in these studies). (B) SEC−MALS data of the ssDNA−pRPA−Rad52 complex. (C) Silver-stained SDS−PAGE (top) and ssDNA detection (bottom) of fractions from panel A: lane 1, Mark12; lanes 2 and 9, input sample, 1.5 $\mu$g loaded; lanes 3−8, peak 1 fractions; lanes 10−17, peak 2 fractions; and lanes 18−20, peak 3 fractions. (D) Detection of ssDNA cross-linked (for 2 min) to protein and separated by SDS−PAGE: lane 1, BlueRanger; lane 2, input sample not cross-linked; lanes 3−5, peak 1 fractions; lanes 6−9, peak 2 fractions; and lanes 10−12, peak 3 fractions. (E) Comparison of the ssDNA affinity of RPA with pRPA. Gel mobility shifts were performed with 0, 3, 30, 75, 150, and 300 fmol of RPA (lanes 1−6) or pRPA (lanes 7−12) with 100 fmol of ssDNA. Line types for SEC−MALS data are as described in the legend of Figure 1.

affinity over that of RPA (Figure 2E). These data suggest that the phosphorylation alone has not disrupted RPA−ssDNA binding but that the protein−protein interactions of pRPA with Rad52 had increased the affinity of Rad52 for ssDNA or caused a conformational change in Rad52 such that the relative ability of the oligonucleotide to be cross-linked is now balanced between Rad52 and pRPA.

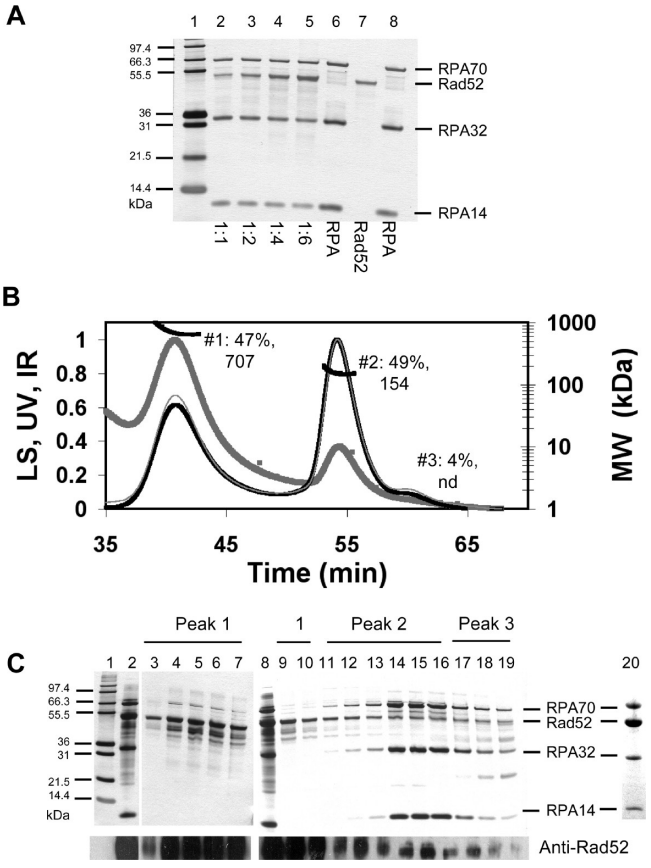


FIGURE 3: Analysis of the RPA−Rad52 complex. (A) Determination of the best mixture for a 1:1 molar ratio of Rad52 to RPA by silver-stained SDS−PAGE. RPA and Rad52 were mixed as indicated on the basis of concentrations determined by the Bio-Rad Bradford protein assay: lane 1, Mark12; lane 2, 1:1; lane 3, 1:2; lane 4, 1:4; lane 5, 1:6; lane 6, RPA, 67 ng; lane 7, Rad52, 28 ng; and lane 8, RPA, 34 ng loaded on gel. (B) SEC−MALS data for the RPA−Rad52 complex. (C) Silver-stained SDS−PAGE (top) and Rad52 Western blot (bottom) of fractions from panel B: lane 1, Mark12; lanes 2 and 8, input sample, 2.8 $\mu$g loaded; lanes 3−7, 9, and 10, peak 1 fractions; lanes 11−16, peak 2 fractions; lanes 17−19, peak 3 fractions; and lane 20, Coomassie blue stain of the input sample. The running positions of Rad52, RPA70, RPA32, and RPA14 are indicated at the right. Line types for SEC−MALS data are as described in the legend of Figure 1.

*RPA−Rad52 Complex Alone*. To help decipher the effects of protein−protein interactions from those of protein−ssDNA interactions in the data given above, the stoichiometry of the RPA−Rad52 complex alone was studied. Rad52 binds Coomassie blue stain very well, causing a relative overestimation of its Bradford concentration relative to RPA; therefore, we used silver-stained gels loaded with various ratios of Rad52 to RPA to find that an approximate equimolar ratio of RPA to Rad52 was formed by mixing RPA and Rad52 in a 1:2 molar ratio (Figure 3A, lane 3, compare staining of RPA70 with Rad52). SEC−MALS analysis defined three species for the RPA−Rad52 mixture (Table 1, sample 3): (1) peak 1, 706.9 kDa aggregates of primarily Rad52 with some RPA [Figure 3C, lanes 3−7, 9, and 10; EM showed some ringlike aggregates (data not shown)], (2) peak 2, 154.4 kDa peak of RPA and some RPA in complex with Rad52 monomer (Figure 3C, lanes 11−16), and (3) peak 3, minor lower-molecular mass species containing RPA and Rad52 (Figure 3C, lanes 17−19). In Figure 3B, peaks 1 and 2 are nearly equally populated (47% vs 49%). Peak 2 may contain a mixture of RPA and a complex of free RPA and Rad52 due to incomplete

separation during SEC. The light scattering signal therefore gives an average of the two masses. Western blot analysis confirmed that Rad52 was present in all fractions. These data indicate that RPA binding to Rad52 can partially break up the Rad52 ring structure.

It is interesting to compare the collection of data from the three types of RPA−Rad52 complexes. Clearly, the breakdown of Rad52 rings to monomers is promoted by prebinding RPA to ssDNA. When the RI peak areas (dark black line) and molecular masses were compared, we observed that the 707 kDa aggregates in peak 1 of Figure 3B disappear and the 142 kDa ssDNA−RPA−monomeric Rad52 complex in peak 3 of Figure 1A becomes the major species (70%). The monomeric form of Rad52 in the complex is further stabilized by the ssDNA−pRPA complex (peak 2, Figure 2B,C), and both proteins now bind the ssDNA (Figure 2D). This indicates that the conformation of Rad52 was changed by the binding of the ssDNA−pRPA complex, and/or the affinity of Rad52 for ssDNA is increased by interaction with the ssDNA−pRPA complex.

*SEC−MALS of Individual Proteins*. As a control and validation of the SEC−MALS technique, the individual proteins and ssDNA−protein complexes were evaluated. Human RPA eluted as a single peak (Figure 4A), and the measured molecular mass (111.0 kDa, 0.4% error) was within 0.2% of predicted values (Table 1, sample 4). RPA was incubated with a mixed sequence 25mer oligonucleotide ($M_W$ = 7815 Da) before SEC−MALS analysis. The ssDNA−RPA complex eluted with a mass (125.1 kDa, 3% error) that best corresponded to a complex of one RPA heterotrimer with two ssDNA molecules bound (Figure 4B and Table 1, sample 5). The corresponding dot blot analysis for ssDNA (Figure 4C) confirms the presence of ssDNA in the peak fractions. The interpretation of this data is limited in that the SEC column used in this study was selected for its large separation range which was useful for the studies with RPA−Rad52 complexes. Therefore, this observation was further studied with an analytical SEC column (Shodex 803) designed for the separation of lower-$M_W$ species (see Figures 1−5 of the Supporting Information). Using this column, a better separation among the ssDNA−RPA complex, free RPA, and free ssDNA was obtained. This gave $M_W$ measurements with smaller errors and better confidence in the measurement. A better understanding of the stoichiometry that exists between RPA and the 25mer ssDNA was gained by varying the molar ratios before SEC−MALS analysis (see discussion in the Supporting Information). These data confirm that the molar ratio mixture used in these studies corresponds to a complex of one RPA heterotrimer with two 25mer ssDNA molecules bound.

Human Rad52 samples eluted primarily as a self-associated complex (Figure 5A, peak 1, 538.9 kDa; Table 1, sample 6). The mass of the self-associated complex corresponds to a ring of 11 Rad52 monomers with the ring structure confirmed by EM (Figure 5B). When combined with ssDNA, the $M_W$ of the major peak of the ssDNA−Rad52 complex corresponds to a complex of 11 Rad52 monomers and 12 ssDNA molecules (Figure 5C, peak 1, 634.9 kDa; Figure 5D, lanes 3−5; Table 1, sample 7). EM of the protein in this peak contained structures of a broken ring assuming a horseshoe-like structure (Figure 5E). The low-$M_W$ second peak of the ssDNA−Rad52 complex contained some Rad52 monomer with an excess of ssDNA (Figure 5C, peak 2; Figure 5D, lanes 6−9). Because of the low concentration and low mass of this species, the light scattering data are weak

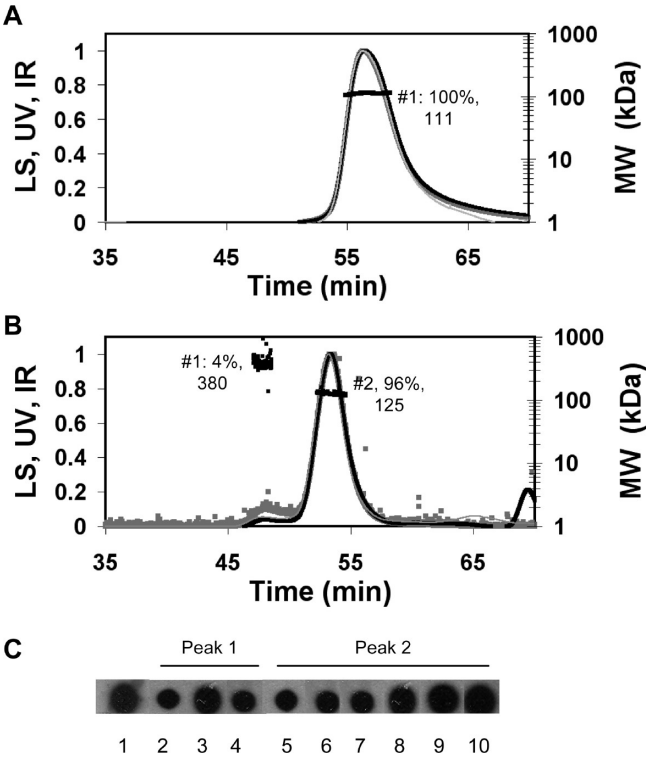


FIGURE 4: Analysis of RPA alone and the ssDNA−RPA complex. (A) SEC−MALS data of RPA alone. (B) SEC−MALS data of the ssDNA−RPA complex. (C) ssDNA levels in ssDNA−RPA fractions of panel B: lane 1, positive control (100 fmol); lanes 2−4, peak 1 fractions; and lanes 5−10, peak 2 fractions. Line types for SEC−MALS data are as described in the legend of Figure 1.

and the $M_W$ could not be determined, but the elution time, ssDNA detection, silver−stained SDS−PAGE, and UV data indicate ssDNA (in excess) and Rad52 monomer are present in peak 2.

To study the end binding capacity of Rad52, we performed gel mobility shift assays with 3′- and 5′-biotin-labeled ssDNA. Gel shifts indicated that as the amount of Rad52 increased and the complex formed, the chemiluminescent signal from the biotin on the ends was quenched by Rad52 binding (Figure 6 of the Supporting Information). This quenching supports end binding by Rad52 under the conditions of this study.

The 25mer ssDNA used was not long enough to cover the predicted footprint of the undecameric Rad52 ring (assuming four nucleotides per Rad52 monomer requires a 44mer). Also, since the ssDNA was in excess, the number of ssDNA ends was relatively large in our system. Therefore, to improve our understanding of the stoichiometry of binding of the ssDNA−Rad52 complex, two molar ratios were studied by SEC−MALS (1:1 and 11:1 ssDNA:ring ratios) using the 25mer (see Figures 8 and 9 of the Supporting Information) and also using a 44mer ssDNA (see Figures 10 and 11 of the Supporting Information). These results are discussed in the supplement and can be summarized as follows. Changing the length of the ssDNA had no effect on the complex, but changing the molar ratio did. At a 1:1 Rad52 ring:ssDNA molar ratio, one molecule of ssDNA was bound to the undecameric Rad52 ring (Table 2 of the Supporting Information, samples 2 and 4). When one ring is mixed with 11 ssDNA molecules, 9−12 ssDNA molecules were bound to the ring (Table 2 of the Supporting Information, samples 3 and 5). Taken together, these data indicate that the mode of ssDNA binding to Rad52 is mainly end binding and that the number of

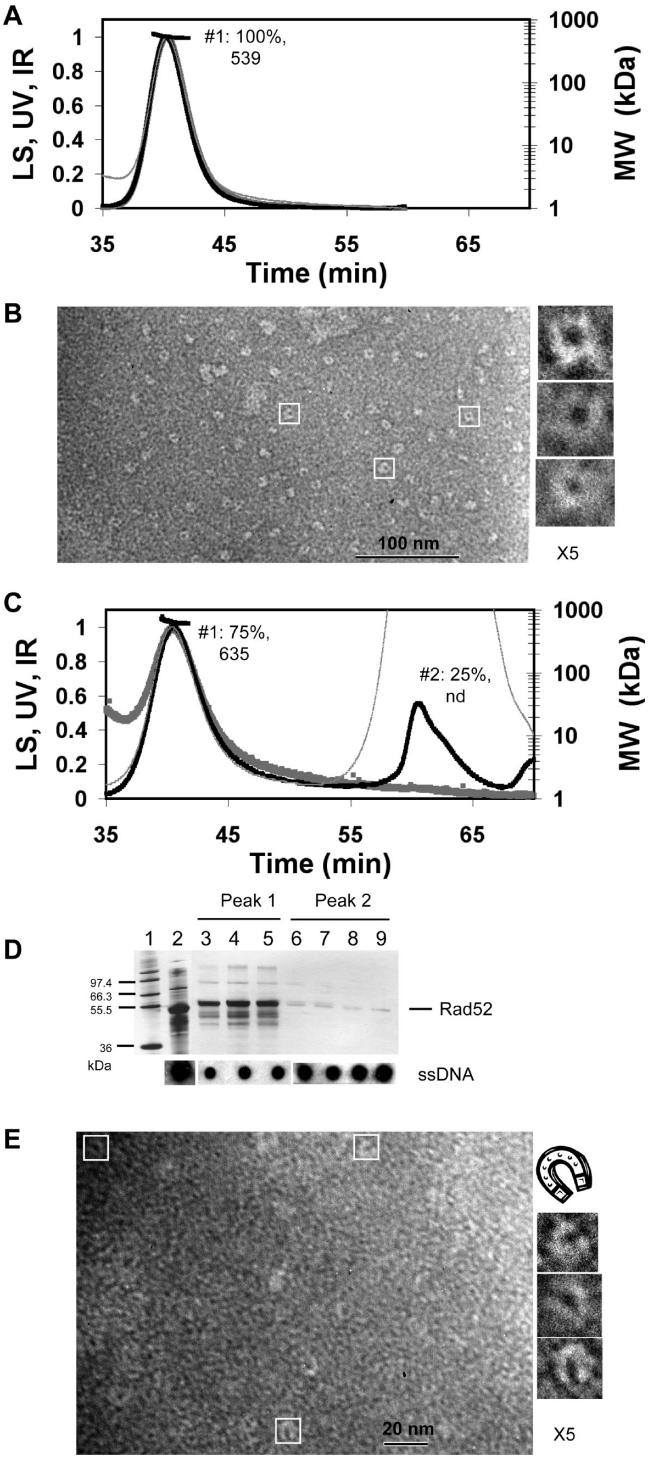


FIGURE 5: Analysis of Rad52 alone and the ssDNA−Rad52 complex. (A) SEC−MALS data of Rad52 alone. (B) EM images of Rad52 from panel A, peak 1 (scale bar, 100 nm). (C) SEC−MALS data of the ssDNA−Rad52 complex. (D) Silver-stained SDS−PAGE (top) and ssDNA detection (bottom) of fractions from panel C: lane 1, Mark12; lane 2, input sample applied to the SEC column; lanes 3−5, peak 1 fractions; and lanes 6−9, peak 2 fractions. (E) EM images of the ssDNA−Rad52 complex from panel C, peak 1 (scale bar, 20 nm). Line types for SEC−MALS data are as described in the legend of Figure 1.

ssDNA molecules bound depends on the number of ssDNA ends available.

## DISCUSSION

The major finding of this study was the effect of phosphorylation of RPA on the ssDNA−RPA−Rad52 complex. Once DSBs are sensed, several downstream HR repair effector proteins are phosphorylated, including RPA. The phosphorylation of the N-terminus of RPA32 in response to DNA-damaging agents has been well documented (*30*, *33*). The form of pRPA used here has been well characterized and is known to be phosphorylated at several more sites other than the N-terminus of RPA32 (*37*, *39*), including the C-terminus of RPA70. These extra sites had no significant effect on nucleotide excision repair (*37*, *39*), and the formation of these new phosphorylation sites by other DNA-damaging agents such as ionizing radiation has not been investigated. Also the effect of this phosphorylated form of RPA on HR-based DSB repair was unknown, so the ssDNA binding and stoichiometry of the ssDNA−pRPA−Rad52 complex were studied in detail here. We found that the ssDNA−pRPA complex efficiently formed a stable complex with monomeric Rad52. Also, Rad52 can be cross-linked with ssDNA but only when RPA is phosphorylated, indicating that the affinity of Rad52 for ssDNA had increased in the pRPA−Rad52 complex. This could also be the result of pRPA causing a conformational change in Rad52 that makes it able to cross-link to ssDNA. This observation provides direct evidence of RPA handing the ssDNA to monomeric Rad52 and a demonstration that this reaction is regulated by the phosphorylation of RPA. A monomeric form of Rad52, as well as the multimeric ring form of Rad52, appears to be relevant to the function of Rad52 in DSB repair. Our earlier experiments with a phosphorylation mimic in which eight Ser/Thr residues on the N-terminus of RPA32 were mutated to Asp indicated that there was no measurable effect on the RPA−Rad52 complex (*62*). Taken together, these results indicate that perhaps the newly identified residues that are phosphorylated on RPA70 may also be important in DSB repair. These observations require further study.

In addition, the stoichiometry of Rad52 rings revealed that purified, full-length, wild-type Rad52 forms a self-associated complex composed of a ring of 11 Rad52 monomers (Figure 5A, peak 1, 539 kDa). This stoichiometry agrees well with the crystal structures for the N-terminal half of Rad52 (*58*, *59*) but disagrees with the heptameric interpretation of earlier wild-type Rad52 EM data (*56*). Further, the binding of ssDNA to Rad52 rings altered Rad52 quaternary structure. The molecular mass of the major species for the ssDNA−Rad52 complex (Figure 5C, peak 1, 635 kDa) best corresponds to a horseshoe-shaped complex of 11 Rad52 monomers and 12 ssDNA molecules. Previous studies and our supplementary data (Figure 6 of the Supporting Information) have shown that Rad52 has a binding preference for 5′ or 3′ ssDNA ends (*50*). Thus, these data could indicate that each Rad52 monomer in the horseshoe is binding to the 3′ or 5′ tail of each ssDNA. When only one molecule of ssDNA is bound, it is likely to be bound at the end by Rad52, but we cannot rule out binding of the rest of the ssDNA molecule in the groove of the undecameric ring as simulated with the apo crystal structure (*54*, *59*). Trace amounts of ssDNA complexed with monomeric Rad52 were also observed in the data (Figure 5C,D, peak 2) which indicates that the binding of ssDNA alone can break up the self-associated Rad52 ring structures when ssDNA is in excess. DNA-induced disassembly of oligomeric forms of hRad52 has also been observed using a native gel electrophoresis analysis (*70*) and atomic force microscopy (*71*).

Our data also shed some light on the formation of a complex of ssDNA, RPA, and Rad52. The number of RPA molecules in a human cell has been estimated to be between $4 \times 10^4$ and $2.4 \times 10^5$ (*72*−*74*), and it is predicted that any ssDNA present in

the cell would be rapidly saturated by RPA binding (*75*). Thus, when Rad52 encounters a ssDNA-tailed substrate at the DSB repair site, it probably already has RPA bound. Experimentally, we observed that RPA and Rad52 form a relatively weak and heterogeneous complex when ssDNA is absent and that the complexes formed become more homogeneous when RPA has ssDNA bound. The major species for the ssDNA−RPA−Rad52 complex incorporated a monomeric form of Rad52. Experimentally, the ssDNA−RPA−Rad52 complex was much more stable than the RPA−Rad52 complex and was easier to measure. Interestingly, RPA is probably in excess over Rad52 in human cells. Although this ratio has not been directly measured in human cells, GFP-tagged proteins in *S. cerevisiae* indicate that there is 4−6 times more RPA than Rad52 (*76*) per yeast cell. Therefore, since the RPA in a cell is likely to be bound to ssDNA and in excess over Rad52, it is unlikely that Rad52 retains its ring structure at the DSB repair site. The disruption of the Rad52 ring structure may be caused by a conformational change in Rad52 structure or may indicate that residues in the so-called self-association region (residues 125−185) are also involved in binding RPA as well as the previously identified RPA binding site that includes residues 220−280 (*61*, *62*). This stoichiometry for the RPA−Rad52 complex at the repair site, which was directly measured here, was previously proposed for *S. cerevisiae* proteins on the basis of the detection of a ssDNA−RPA−Rad52 complex in gel mobility shift assays (*77*). While our studies confirm this stoichiometry, they also provide the molecular mass of the complex, which cannot be measured with native gels. These observations are also in agreement with the work of Navadgi and co-workers, who observed monomeric complexes of human Rad51, Rad52, and ssDNA (*78*).

*A Model for the Early Steps in Homologous Recombination-Based DSB Repair*. The main conclusions of this study are that the active form of Rad52 is monomeric, Rad52 forms a monomeric complex with RPA, and complex formation is promoted when RPA has ssDNA bound and is phosphorylated. Finally, phosphorylation of RPA enhances Rad52's ability to bind ssDNA through either an induced conformational change, an increase in binding affinity, or both. Based on these observations, we propose the following model for the initial steps of HR-based DSB repair. After the DSB is formed (Figure 6A) and resected by the Rad50−Mre11−NBS1 complex to form ssDNA tails, RPA binds the ssDNA tightly and removes any secondary structure (Figure 6B). Rad52 binding to RPA at this stage would not promote DSB repair as the affinity of RPA for ssDNA is increased by formation of this complex (this work and ref *62*). Several DNA repair proteins become phosphorylated when repair is needed, and during the cellular DNA damage response, RPA becomes phosphorylated (Figure 6C). Phosphorylated RPA with ssDNA bound also efficiently forms a complex with monomeric Rad52. Intermediate structures include various multimers of Rad52 bound to the ssDNA−pRPA complex (Figure 6D). The predominant monomeric ssDNA−pRPA−Rad52 complex is formed (Figure 6D), and then ssDNA−Rad52 monomeric complexes form as the affinity of Rad52 for ssDNA is realized (Figure 6E). These ssDNA tails with phosphorylated RPA and monomeric Rad52 bound are ready for further processing by Rad51-mediated DSB repair or single-strand annealing-based repair. The steps in this model will be tested in future studies.

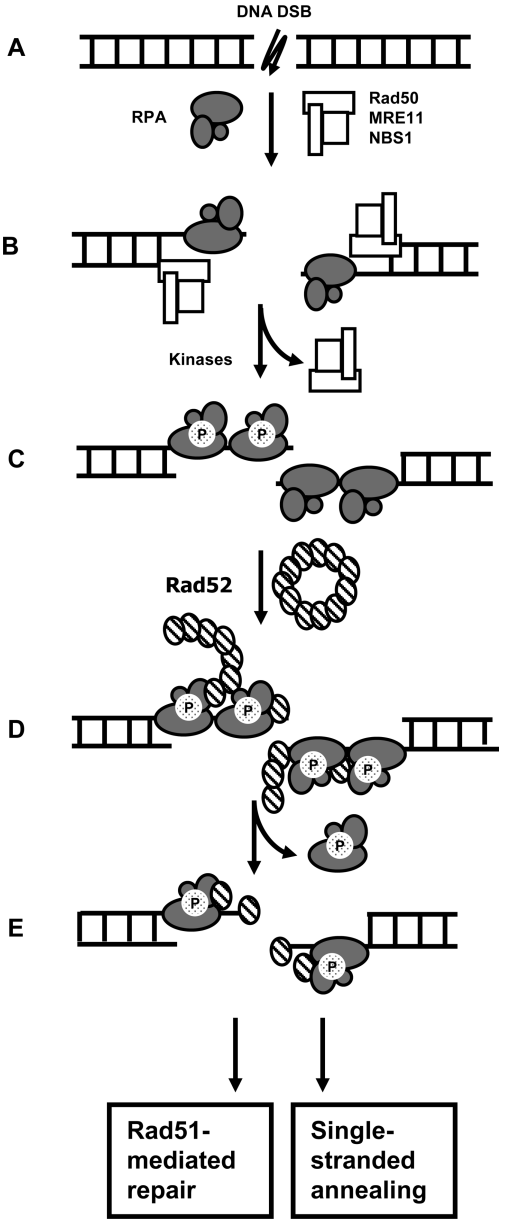


FIGURE 6: Concluding model for the initial steps of HR-based DSB repair pathways.

## ACKNOWLEDGMENT

We are grateful to the staff at Wyatt Technology Corp. for their helpful advice; in particular, we thank Andy Meyer and William Wittbold for useful discussions. We thank Doba Jackson and Uffe H. Mortensen for helpful discussions, Jeff Lovelace and Kerry Brader for technical assistance, and Tom Barger for assistance with samples at the University of Nebraska Medical Center Core Electron Microscopy Research Facility.

## SUPPORTING INFORMATION AVAILABLE

Additional experimental procedures, results, and discussion.

This material is available free of charge via the Internet at http://pubs.acs.org.

## REFERENCES

1. Shinohara, A., and Ogawa, T. (1995) Homologous recombination and the roles of double-strand breaks. *Trends Biochem. Sci. 20*, 387–391.

2. Krogh, B. O., and Symington, L. S. (2004) Recombination proteins in yeast. *Annu. Rev. Genet. 38*, 233–271.
3. Sung, P., Trujillo, K. M., and Van Komen, S. (2000) Recombination factors of *Saccharomyces cerevisiae*. *Mutat. Res. 451*, 257–275.
4. Sung, P. (1997) Function of yeast Rad52 protein as a mediator between replication protein A and the Rad51 recombinase. *J. Biol. Chem. 272*, 28194–28197.
5. Shinohara, A., and Ogawa, T. (1998) Stimulation by Rad52 of yeast Rad51-mediated recombination. *Nature 391*, 404–407.
6. New, J. H., Sugiyama, T., Zaitseva, E., and Kowalczykowski, S. C. (1998) Rad52 protein stimulates DNA strand exchange by Rad51 and replication protein A. *Nature 391*, 407–410.
7. Sugiyama, T., New, J. H., and Kowalczykowski, S. C. (1998) DNA annealing by RAD52 protein is stimulated by specific interaction with the complex of replication protein A and single-stranded DNA. *Proc. Natl. Acad. Sci. U.S.A. 95*, 6049–6054.
8. Benson, F. E., Baumann, P., and West, S. C. (1998) Synergistic actions of Rad51 and Rad52 in recombination and DNA repair. *Nature 391*, 401–404.
9. Baumann, P., and West, S. C. (1999) Heteroduplex formation by human Rad51 protein: Effects of DNA end-structure, hRP-A and hRad52. *J. Mol. Biol. 291*, 363–374.
10. McIlwraith, M. J., Van Dyck, E., Masson, J. Y., Stasiak, A. Z., Stasiak, A., and West, S. C. (2000) Reconstitution of the strand invasion step of double-strand break repair using human Rad51 Rad52 and RPA proteins. *J. Mol. Biol. 304*, 151–164.
11. Sung, P., Krejci, L., Van Komen, S., and Sehorn, M. G. (2003) Rad51 recombinase and recombination mediators. *J. Biol. Chem. 278*, 42729–42732.
12. Beernink, H. T., and Morrical, S. W. (1999) RMPs: Recombination/replication mediator proteins. *Trends Biochem. Sci. 24*, 385–389.
13. McIlwraith, M. J., and West, S. C. (2008) DNA repair synthesis facilitates RAD52-mediated second-end capture during DSB repair. *Mol. Cell 29*, 510–516.
14. Kowalczykowski, S. C. (2005) Cancer: Catalyst of a catalyst. *Nature 433*, 591–592.
15. Iftode, C., Daniely, Y., and Borowiec, J. A. (1999) Replication Protein A (RPA): The Eukaryotic SSB. *Crit. Rev. Biochem. Mol. Biol. 34*, 141–180.
16. Wold, M. S. (1997) RPA: A Heterotrimeric, Single-Stranded DNA-Binding Protein Required for Eukaryotic DNA Metabolism. *Annu. Rev. Biochem. 66*, 61–91.
17. Loo, Y.-M., and Melendy, T. (2000) The majority of human replication protein A remains complexed throughout the cell cycle. *Nucleic Acids Res. 28*, 3354–3360.
18. Dimitrova, D. S., and Gilbert, D. M. (2000) Stability and Nuclear Distribution of Mammalian Replication Protein A Heterotrimeric Complex. *Exp. Cell Res. 254*, 321–327.
19. Fairman, M. P., and Stillman, B. (1988) Cellular Factors Required for Multiple Stages of SV40 DNA Replication in Vitro. *EMBO J. 7*, 1211–1218.
20. Kim, C., Paulus, B. F., and Wold, M. S. (1994) Interactions of Human Replication Protein A with Oligonucleotides. *Biochemistry 33*, 14197–14206.
21. Fanning, E., Klimovich, V., and Nager, A. R. (2006) A dynamic model for replication protein A (RPA) function in DNA processing pathways. *Nucleic Acids Res. 34*, 4126–4137.
22. Gomes, X. V., Henricksen, L. A., and Wold, M. S. (1996) Proteolytic Mapping of Human Replication Protein A: Evidence for Multiple Structural Domains and a Conformational Change upon Interaction with Single-stranded DNA. *Biochemistry 35*, 5587–5594.
23. Blackwell, L., Borowiec, J., and Mastrangelo, I. (1996) Single-Stranded DNA Binding Alters Human Replication Protein A Structure and Facilitates Interaction with DNA-Dependent Protein Kinase. *Mol. Cell. Biol. 16*, 4798–4807.
24. Wu, X., Yang, Z., Liu, Y., and Zou, Y. (2005) Preferential localization of hyperphosphorylated replication protein A to double-strand break repair and checkpoint complexes upon DNA damage. *Biochem. J. 391*, 473–480.
25. Zhou, B. B., and Elledge, S. J. (2000) The DNA damage response: Putting checkpoints in perspective. *Nature 408*, 433–439.
26. Niu, H., Erdjument-Bromage, H., Pan, Z., Lee, S., Tempst, P., and Hurwitz, J. (1997) Mapping of amino acid residues in the p34 subunit of human single-stranded DNA-binding protein phosphorylated by DNA-dependent protein kinase and cdc2 kinase in vitro. *J. Biol. Chem. 272*, 12634–12641.
27. Zernik-Kobak, M., Vasunia, K., Connelly, M., Anderson, C. W., and Dixon, K. (1997) Sites of UV-induced Phosphorylation of the p34 Subunit of Replication Protein A from HeLa Cells. *J. Biol. Chem. 272*, 23896–23904.
28. Binz, S. K., Sheehan, A. M., and Wold, M. S. (2004) Replication protein A phosphorylation and the cellular response to DNA damage. *DNA Repair 3*, 1015–1024.
29. Treuner, K., Okuyama, A., Knippers, R., and Fackelmayer, F. O. (1999) Hyperphosphorylation of replication protein A middle subunit (RPA32) in apoptosis. *Nucleic Acids Res. 27*, 1499–1504.
30. Liu, V. F., and Weaver, D. T. (1993) The ionizing radiation-induced Replication Protein A phosphorylation response differs between ataxia telangiectasia and normal human cells. *Mol. Cell. Biol. 13*, 7222–7231.
31. Fang, F., and Newport, J. W. (1993) Distinct Roles of cdk2 and cdc2 in RP-A Phosphorylation During the Cell Cycle. *J. Cell Sci. 106*, 983–994.
32. Din, S.-U., Brill, S. J., Fairman, M. P., and Stillman, B. (1990) Cell cycle regulated phosphorylation of DNA replication factor A from human and yeast cells. *Genes Dev. 4*, 968–977.
33. Carty, M. P., Zernik-Kobak, M., McGrath, S., and Dixon, K. (1994) UV light-induced DNA synthesis arrest in HeLa cells is associated with changes in phosphorylation of human single-stranded DNA-binding protein. *EMBO J. 13*, 2114–2123.
34. Treuner, K., Findeisen, M., Strausfeld, U., and Knippers, R. (1999) Phosphorylation of Replication Protein A Middle Subunit (RPA32) Leads to a Disassembly of the RPA Heterotrimer. *J. Biol. Chem. 274*, 15556–15561.
35. Block, W. D., Yu, Y., and Lees-Miller, S. P. (2004) Phosphatidyl inositol 3-kinase-like serine/threonine protein kinases (PIKKs) are required for DNA damage-induced phosphorylation of the 32 kDa subunit of replication protein A at threonine 21. *Nucleic Acids Res. 32*, 997–1005.
36. Anantha, R. W., Vassin, V. M., and Borowiec, J. A. (2007) Sequential and synergistic modification of human RPA stimulates chromosomal DNA repair. *J. Biol. Chem. 282*, 35910–35923.
37. Nuss, J. E., Patrick, S. M., Oakley, G. G., Alter, G. M., Robison, J. G., Dixon, K., and Turchi, J. J. (2005) DNA damage induced hyperphosphorylation of replication protein A. 1. Identification of novel sites of phosphorylation in response to DNA damage. *Biochemistry 44*, 8428–8437.
38. Oakley, G. G., Patrick, S. M., Yao, J., Carty, M. P., Turchi, J. J., and Dixon, K. (2003) RPA phosphorylation in mitosis alters DNA binding and protein-protein interactions. *Biochemistry 42*, 3255–3264.
39. Patrick, S. M., Oakley, G. G., Dixon, K., and Turchi, J. J. (2005) DNA damage induced hyperphosphorylation of replication protein A. 2. Characterization of DNA binding activity, protein interactions, and activity in DNA replication and repair. *Biochemistry 44*, 8438–8448.
40. Sleeth, K. M., Sorensen, C. S., Issaeva, N., Dziegielewski, J., Bartek, J., and Helleday, T. (2007) RPA mediates recombination repair during replication stress and is displaced from DNA by checkpoint signalling in human cells. *J. Mol. Biol. 373*, 38–47.
41. Sugiyama, T., Kantake, N., Wu, Y., and Kowalczykowski, S. C. (2006) Rad52-mediated DNA annealing after Rad51-mediated DNA strand exchange promotes second ssDNA capture. *EMBO J. 25*, 5539–5548.
42. Gudmundsdottir, K., and Ashworth, A. (2006) The roles of BRCA1 and BRCA2 and associated proteins in the maintenance of genomic stability. *Oncogene 25*, 5864–5874.
43. Paques, F., and Haber, J. E. (1999) Multiple pathways of recombination induced by double-strand breaks in *Saccharomyces cerevisiae*. *Microbiol. Mol. Biol. Rev. 63*, 349–404.
44. Larminat, F., Germanier, M., Papouli, E., and Defais, M. (2002) Deficiency in BRCA2 leads to increase in non-conservative homologous recombination. *Oncogene 21*, 5188–5192.
45. Tutt, A., Bertwistle, D., Valentine, J., Gabriel, A., Swift, S., Ross, G., Griffin, C., Thacker, J., and Ashworth, A. (2001) Mutation in Brca2 stimulates error-prone homology-directed repair of DNA double-strand breaks occurring between repeated sequences. *EMBO J. 20*, 4704–4716.
46. Navadgi, V. M., Dutta, A., and Rao, B. J. (2003) Human Rad52 facilitates a three-stranded pairing that follows no strand exchange: A novel pairing function of the protein. *Biochemistry 42*, 15237–15251.
47. Ristic, D., Modesti, M., Kanaar, R., and Wyman, C. (2003) Rad52 and Ku bind to different DNA structures produced early in double-strand break repair. *Nucleic Acids Res. 31*, 5229–5237.
48. Kagawa, W., Kagawa, A., Saito, K., Ikawa, S., Shibata, T., Kurumizaka, H., and Yokoyama, S. (2008) Identification of a second DNA binding site in the human Rad52 protein. *J. Biol. Chem. 283*, 24264–24273.

49. Van Dyck, E., Stasiak, A. Z., Stasiak, A., and West, S. C. (1999) Binding of double-strand breaks in DNA by human Rad52 protein. *Nature 398*, 728–731.
50. Parsons, C. A., Baumann, P., Van Dyck, E., and West, S. C. (2000) Precise binding of single-stranded DNA termini by human RAD52 protein. *EMBO J. 19*, 4175–4181.
51. Wu, Y., Siino, J. S., Sugiyama, T., and Kowalczykowski, S. C. (2006) The DNA binding preference of RAD52 and RAD59 proteins: Implications for RAD52 and RAD59 protein function in homologous recombination. *J. Biol. Chem. 281*, 40001–40009.
52. Lloyd, J. A., Forget, A. L., and Knight, K. L. (2002) Correlation of biochemical properties with the oligomeric state of human rad52 protein. *J. Biol. Chem. 277*, 46172–46178.
53. Shinohara, A., Shinohara, M., Ohta, T., Matsuda, S., and Ogawa, T. (1998) Rad52 forms ring structures and cooperates with RPA in single-strand DNA annealing. *Genes Cells 3*, 145–156.
54. Van Dyck, E., Hajibagheri, N. M. A., Stasiak, A., and West, S. C. (1998) Visualisation of Human Rad52 Protein and its Complexes with hRad51 and DNA. *J. Mol. Biol. 284*, 1027–1038.
55. Kagawa, W., Kurumizaka, H., Ikawa, S., Yokoyama, S., and Shibata, T. (2001) Homologous Pairing Promoted by the Human Rad52 Protein. *J. Biol. Chem. 276*, 35201–35208.
56. Stasiak, A. Z., Larquet, E., Stasiak, A., Muller, S., Engel, A., Dyck, E. V., West, S. C., and Egelman, E. H. (2000) The human Rad52 protein exists as a heptameric ring. *Curr. Biol. 10*, 337–340.
57. Ranatunga, W., Jackson, D., Lloyd, J. A., Forget, A. L., Knight, K. L., and Borgstahl, G. E. O. (2001) Human Rad52 Exhibits Two Modes of Self-association. *J. Biol. Chem. 276*, 15876–15880.
58. Kagawa, W., Kurumizaka, H., Ishitani, R., Fukai, S., Nureki, O., Shibata, T., and Yokoyama, S. (2002) Crystal structure of the homologous-pairing domain from the human Rad52 recombinase in the undecameric form. *Mol. Cell 10*, 359–371.
59. Singleton, M. R., Wentzell, L. M., Liu, Y., West, S. C., and Wigley, D. B. (2002) Structure of the single-strand annealing domain of human RAD52 protein. *Proc. Natl. Acad. Sci. U.S.A. 99*, 13492–13497.
60. Plate, I., Albertsen, L., Lisby, M., Hallwyl, S. C., Feng, Q., Seong, C., Rothstein, R., Sung, P., and Mortensen, U. H. (2008) Rad52 multimerization is important for its nuclear localization in *Saccharomyces cerevisiae*. *DNA Repair 7*, 57–66.
61. Park, M. S., Ludwig, D. L., Stigger, E., and Lee, S. H. (1996) Physical interaction between Human RAD52 and RPA is Required for Homologous Recombination in Mammalian Cells. *J. Biol. Chem. 271*, 18996–19000.
62. Jackson, D., Dhar, K., Wahl, J. K., Wold, M. S., and Borgstahl, G. E. (2002) Analysis of the human replication protein A:Rad52 complex: Evidence for crosstalk between RPA32, RPA70, Rad52 and DNA. *J. Mol. Biol. 321*, 133–148.
63. Mer, G., Bochkarev, A., Gupta, R., Bochkareva, E., Frappier, L., Ingles, C. J., Edwards, A. M., and Chazin, W. J. (2000) Structural Basis for the Recognition of DNA Repair Proteins UNG2, XPA and Rad52 by Replication Factor RPA. *Cell 103*, 449–456.
64. Hays, S. L., Firmenich, A. A., Massey, P., Banerjee, R., and Berg, P. (1998) Studies of the Interaction between Rad52 Protein and the Yeast Single-Stranded DNA Binding Protein RPA. *Mol. Cell. Biol. 18*, 4400–4406.
65. Seong, C., Sehorn, M. G., Plate, I., Shi, I., Song, B., Chi, P., Mortensen, U., Sung, P., and Krejci, L. (2008) Molecular anatomy of the recombination mediator function of *Saccharomyces cerevisiae* Rad52. *J. Biol. Chem. 283*, 12166–12174.
66. Plate, I., Hallwyl, S. C., Shi, I., Krejci, L., Muller, C., Albertsen, L., Sung, P., and Mortensen, U. H. (2008) Interaction with RPA is necessary for Rad52 repair center formation and for its mediator activity. *J. Biol. Chem. 283*, 29077–29085.
67. Tarazona, M. P., and Saiz, E. (2003) Combination of SEC/MALS experimental procedures and theoretical analysis for studying the solution properties of macromolecules. *J. Biochem. Biophys. Methods 56*, 95–116.
68. Mogridge, J. (2004) Using light scattering to determine the stoichiometry of protein complexes. *Methods Mol. Biol. 261*, 113–118.
69. Henricksen, L. A., Umbricht, C. B., and Wold, M. S. (1994) Recombinant Replication Protein A: Expression, Complex Formation and Function Characterization. *J. Biol. Chem. 269*, 11121–11132.
70. Navadgi, V. M., Shukla, A., and Rao, B. J. (2005) Effect of DNA sequence and nucleotide cofactors on hRad51 binding to ssDNA: Role of hRad52 in recruitment. *Biochem. Biophys. Res. Commun. 334*, 696–701.
71. D'Souza, J. S., Dharmadhikari, J. A., Dharmadhikari, A. K., Navadgi, V., Mathur, D., and Rao, B. J. (2006) Human Rad52 binding reders ssDNA unfolded: Image and contour length analysis by atomic force microscopy. *Curr. Sci. 91*, 1641–1648.
72. Wold, M. S., and Kelly, T. (1988) Purification and Characterization of Replication protein A, a Cellular Protein Required for in vitro Replication of Simian Virus 40 DNA. *Proc. Natl. Acad. Sci. U.S.A. 85*, 2523–2527.
73. Kenny, M. K., Schlegel, U., Furneaux, H., and Hurwitz, J. (1990) The Role of Human Single-stranded DNA Binding Protein and Its Individual Subunits in Simian Virus 40 DNA Replication. *J. Biol. Chem. 265*, 7693–7700.
74. Seroussi, E., and Lavi, S. (1993) Replication protein A is the major single-stranded DNA binding protein detected in mammalian cell extracts by gel retardation assays and UV cross-linking of long and short single-stranded DNA molecules. *J. Biol. Chem. 268*, 7147–7154.
75. Kim, C., and Wold, M. S. (1995) Recombinant Human Replication Protein A Binds to Polynucleotides with Low Cooperativity. *Biochemistry 34*, 2058–2064.
76. Ghaemmaghami, S., Huh, W. K., Bower, K., Howson, R. W., Belle, A., Dephoure, N., O'Shea, E. K., and Weissman, J. S. (2003) Global analysis of protein expression in yeast. *Nature 425*, 737–741.
77. Sugiyama, T., and Kowalczykowski, S. C. (2002) Rad52 protein associates with replication protein A (RPA)-single-stranded DNA to accelerate Rad51-mediated displacement of RPA and presynaptic complex formation. *J. Biol. Chem. 277*, 31663–31672.
78. Navadgi, V. M., Shukla, A., Vempati, R. K., and Rao, B. J. (2006) DNA mediated disassembly of hRad51 and hRad52 proteins and recruitment of hRad51 to ssDNA by hRad52. *FEBS J. 273*, 199–207.